Label-free quantitative proteomic analysis of the inhibition effect of *Lactobacillus rhamnosus* GG on *Escherich coli* biofilm formation in coculture

Huiyi Song (songhuiyi@dmu.edu.cn)
First Affiliated Hospital of Dalian Medical University
Ni Lou
Dalian Medical University
Jianjun Liu
First Affiliated Hospital of Dalian Medical University
Hong Xiang
First Affiliated Hospital of Dalian Medical University
Dong Shang
First Affiliated Hospital of Dalian Medical University

Research article

Keywords: label-free quantitative proteomics, coculture, Lactobacillus rhamnosus GG micro-capsules, mechanism

Posted Date: March 13th, 2020

DOI: https://doi.org/10.21203/rs.3.rs-17189/v1

Abstract

Background: *Escherich coli* (*E.coli*) is the principal pathogen that causes biofilm formation; the latter is associated with infectious diseases and antibiotic resistance. In our previous work, we demonstrated that probiotic microcapsules have superior biofilm inhibition capacity compared to probiotic sterile culture supernatant. Herein, the mechanism of the inhibition effects was investigated using label-free quantitative proteomics analysis.

Results: The proteomic analysis characterized a total of 1655 proteins in *E.coli* K12MG1655 and 1431 proteins in *Lactobacillus rhamnosus* GG (LGG). Among them, after coculture treatment, there were 262 and differentially expressed proteins that were specific for *E.coli* and 291 for LGG. The differentially expressed proteins after coculture were related to cellular metabolism, the stress response, transcription, and the cell membrane. In addition, we identified five strain-specific genes in *E.coli* and LGG, respectively, which were consistent with the proteomics results.

Conclusions: These findings indicate that LGG microcapsules may inhibit *E.coli* biofilm inhibition by disrupting metabolic processes, particularly in relation to energy metabolism and stimulus responses, both of which are critical for the growth of LGG. Together, these findings increase our understanding of the interactions between bacteria under coculture conditions.

Background

Biofilms are complex bacterial community structures that can attach to a surface. They are connected to this surface via extracellular polymeric substances (EPS) which form a matrix composed primarily of polysaccharides, proteins, and DNA; this encapsulates the bacteria [1]. Biofilms not only cause economic losses, but also present a public health hazard. This is because the bacteria present within biofilms are much more resistant to antibiotics, disinfectants [2], and the host immune system effectors [3]. Therefore, it is critical to uncover effective non-toxic, or less toxic, antifungal agents with novel modes of action.

A recent study suggested that probiotic supernatants have antipathogenic properties [4], which implies that probiotics may inhibit biofilm formation through cell-cell communication. However, there has been little progress in this field to date. In our previous study, bacteria immobilized in microcapsules showed superior biofilm inhibition capacity compared to probiotic sterile culture supernatant. As a result, we established a Lactobacillus rhamnosus GG (LGG) microcapsule-planktonic Escherich coli (E.coli) coculture model and evaluated the biofilm inhibition effect [5].

Proteomics analysis combined with bioinformatics tools has emerged as an important approach to extract detailed information on cellular regulatory mechanisms at the protein level. In this study, we aimed to investigate the modulatory effects of LGG microcapsules on the E.coli proteome. To this end, a label-free quantitative proteomic approach was used to identify proteins with significantly changed expression profiles, in order to confirm their functions in LGG-treated E.coli. Ultimately, these findings will further our understanding of the possible molecular action of probiotic microcapsules against pathogen

biofilm formation and provide a powerful platform for future mechanistic studies of bacterial interactions.

Results

The inhibition effect of LGG microcapsules on E.coli biofilm formation

The biofilms formed by coculture and pure culture were stained with SYTO-9 (20 mM) for 15 min at room temperature and were analyzed by confocal microscopy (Leica SP8, Germany) at 480 nm (excitation) (Fig. 1). The observed reduction in the intensity of fluorescence provides evidence of biofilm inhibition.

Global proteomic survey of LGG and E.coli before and after coculture treatment

In this study, we evaluated E.coli in the biofilm functional genome at the proteome level in response to LGG microcapsules, before and after coculture. The experiments were performed in biological triplicates. Proteins from total bacterial lysates were extracted and digested in solution. Then, the resulting peptides were analyzed using the LC/MS^E approach [6]. A total of 1655 and 1431 bacterial proteins were identified in E.coli and LGG, respectively. Differential expression was considered only for proteins that were significantly different with an ANOVA p-value < 0.05 and with at least a 2-fold change (cut-off value). Based on these parameters, 19 proteins were identified before coculture in E.coli, but not identified after coculture, and 68 proteins were not identified before coculture in E.coli., but identified after coculture. For LGG, these values were 35 and 15, respectively (Fig. 2a). Hierarchical cluster analysis was performed for the coculture group and the control group (Fig. 2b). As shown in Fig. 2b, the differentially expressed proteins in the coculture group did not cluster together with the ones in the control group.

Functional categorization of proteomes of E.coli and LGG before and after coculture

Following the label-free quantification analysis, the functions of the regulated bacterial proteins were enriched according to Gene Ontology (GO) terms, with their redundant GO terms summarized and unified. For E.coli, 262 proteins were differentially expressed after co-culture, among which 31 proteins were up-regulated in the presence of LGG microcapsules and 231 were down-regulated. The number of up-regulated and down-regulated proteins for LGG was 104 and 187, respectively (Table 1).

Table 1
Numbers of the proteins significantly up-regulated/down-regulated after coculture treatment in E.coli and LGG by GO analysis.

Strains	Comparisons (Before coculture/After coculture)	
	Up-regulated proteins	Down-regulated proteins
E.coli	31	231
LGG	104	187

Functional categorization of E.coli proteome before and after coculture

A total of 358, 356, and 50 GO terms for molecular function, biological process, and cellular component, respectively, were generated based upon the up-regulated proteins in E.coli after coculture. Based upon the down-regulated proteins, a total of 56, 57, and 26 GO terms were generated. Among the GO terms for biological process, “cellular response to DNA damage stimulus” (22.75%) was the most common function in up-regulated proteins in the E.coli coculture group. Among the GO terms for cellular component, the most common up-regulated proteins belonged to “cytosol” (33.86%), while the most common down-regulated proteins belonged to “plasma membrane” (12.58%). For molecular function, 13.51% of up- and 11.69% of down-regulated proteins were related to “4 iron, 4 sulfur cluster binding” and “ATPase activity”, respectively (Fig. 3).

Functional categorization of LGG proteome before and after coculture

A total of 211, 138, and 20 GO terms for molecular function, biological process, and cellular component, respectively, were generated. Furthermore, 85, 50, and 10 GO terms, respectively, belonged to up-regulated proteins in LGG after coculture, while 150, 102, and 15 GO terms, respectively, belonged to down-regulated proteins. Among the GO terms for biological process, “carbohydrate metabolic process” (22.75%) was the most common function in up-regulated proteins in the coculture group. Among the GO terms for cellular component, the most common up-regulated proteins belonged to “cytoplasm” (33.86%), while the most common down-regulated proteins belonged to “ATP binding” (12.58%). For molecular function, 17.92% of up- and 16.55% of down-regulated proteins were related to “oxidoreductase activity” and “structural constituent of ribosome”, respectively (Fig. 3).

E.coli and LGG affect the mRNA levels of each other’s target proteins in the coculture model

The proteomics analysis identified differential regulation of several proteins in E.coli and LGG microcapsule coculture (Supplementary Table S1 and S2). We then performed real-time RT-PCR analysis of select targets to validate the observed differential protein levels (Fig. 4). In line with the findings from the global proteomics analysis, we observed increased bioD2, panD, and ygiW mRNA levels in E.coli. We also quantified the mRNA levels of bamE and dnaK, which encode down-regulated expression at the

transcription level. Additionally, given the extensive effect of LGG microcapsules on biofilm inhibition, we determined that the mRNA expression levels of purD and purM were up-regulated 3.1-fold and 7.3-fold, respectively. The mRNA levels of murB, murF, and ackA were also decreased after coculture with E.coli for 48 h.

Discussion

Biofilm formation is associated with resistance to antibiotic therapy, and thus, continues to be a major health threat in both hospital and community settings [7][8]. We previously reported that probiotic LGG microcapsules could inhibit E.coli biofilm formation without causing antibiotic resistance. Probiotics have many benefits for human health and are used both therapeutically and in the food industry [9]. These findings prompted us to evaluate the mechanism of action underlying the inhibitory effect of LGG microcapsules on antibacterial biofilm formation.

Effects of LGG microcapsules on the growth and metabolism of E.coli in coculture

Our proteomic analysis detected a difference between the differentially expressed proteins of E.coli before and after coculture; these differences were related to cellular response to DNA damage stimulus and cell wall organization. Thus, these findings indicate that the proteins involved in responses to the environment have changed during coculture. From this point of view, we focus on the stress response of E.coli in the coculture model. First, we observed increased mRNA levels of the bioD2 gene. The bioD2 protein is an ATP-dependent dethiobiotin synthetase that encodes a homolog of dethiobiotin synthetase, which is a penultimate enzyme in the biotin synthesis pathway. Thus, it is likely that such up-regulated expression in the presence of LGG microcapsules enhanced the degraders requirement for biotin, which is synthesized de novo under the conditions of acid, osmotic, and oxidative stresses with the involvement of different isozymes. This explanation is supported by the up-regulated expression in both the proteomics and RT-PCR analyses, and is further validated by the inhibition effect of LGG microcapsules on E.coli biofilm formation.

Aspartate 1-decarboxylase (PanD) is the only enzyme capable of β-alanine synthesis in E. coli. In bacteria, fungi, and plants, β-alanine is a precursor to pantothenate, which in turn is a required metabolite for the synthesis of coenzyme A (CoA) in all organisms [10]. Research indicates that chloroplast engineering of the beta-alanine pathway by over-expression of E. coli panD enhances thermotolerance of photosynthesis and biomass production following high temperature stress [11].

During the coculture process, E.coli strains are frequently confronted by acid stress produced by LGG metabolism. The ygiW protein is reported to be involved in the stress response associated with exposure to H_2O_2, cadmium, and acid [12]. An earlier study also reported that expression of functional YgiW and QseC proteins is necessary for optimal biofilm growth of A. actinomycetemcomitans [13]. When we compared the expression levels of the ygiW gene between LGG microcapsules and coculture conditions, we observed 4.0-fold change ratios.

The proteomics analysis revealed that several virulence-related proteins, such as bamE and dnaK, were down-regulated when E.coli was treated with LGG microcapsules. The most down-regulated protein, bamE (MHC class II analog protein, Log2FC=-9.2), is an integral outer membrane β-barrel protein (OMP) that is assembled by the beta-barrel assembly machine (Bam) complex in Gram-negative bacteria [14]. Another down-regulated protein, DanK, is an important factor in all three antibiotic-related persister formation pathways. The decreased persistence phenotype, as well as the growth defect of dnaK, seems to depend on functional (p)ppGpp [15]. Heterogeneous expression of the dnaKgene from A. acidoterrestris can significantly enhance the resistance of host bacteria E. coliagainst heat and acid stresses [16]. Furthermore, the DnaK-DnaJ-GrpE chaperone machine plays an important role in cell physiology, including E.coli biofilm development [17].

Effects of E.coli on the growth and metabolism of LGG microcapsules in coculture

Proteomics analysis indicated that E.coli coculture with LGG microcapsules elicited a cellular response in LGG and E.coli strains which is related to a certain intracellular mechanism. Coculture with LGG microcapsules places environmental stress on E.coli and this in turn raises a cellular response in LGG as well [18]. For LGG, the possible responses to the E.coli coculture include physiological and developmental changes, reprogramming of the resistance gene or proteins, and alterations to the way in which energy is supplemented. Proteomics analysis revealed that coculture with E.coli significantly up-regulated two nucleotide metabolism-related genes, purD and purM. The pur-operon (purEKCSQLFMNHD) is responsible for the catalysis of de novo synthesis of inosine monophosphate (IMP) from phosphoribosyl pyrophosphate [19]. In S. aureus, purine biosynthesis enzymes have been closely implicated in virulence, persistence, and tolerance to stresses such as antibiotic resistance [20][21]. Such extensive effects could be attributed to the potential modulation of the transcription of the operon by bacteria secreted extracellular compounds. In another study, purD and purF mutants were constructed in macrophage-like RAW264.7 and HeLa cells. The purD and purF mutants showed significantly decreased intracellular survival, and complementation of these mutants with intact copies of purD or purF genes of Brucella abortus strain RB51 restored these defects. These findings suggest that genes encoding the early stages of purine biosynthesis (purD and purF) are required for intracellular survival and virulence of the RB51 strain [22]. Thus, it may be that LGG strains maintain intracellular survival and homeostasis by up-regulating purD and purM genes.

Coculture of LGG microcapsules with E.coli appeared to down-regulate murB gene expression and to completely abolish expression of the murF gene. Bacteria generally synthesize their own active form of N-acetylmuramic acid, UDP-N-acetylmuramic acid [23], and the MurB enzyme (UDP-N-acetylglucosamine pyruvate enol ether reductase) plays an important role in the biosynthesis of this substance [24]. The MurB enzyme converts UDP-N-acetylglucosamine pyruvate enol ether to UDP-N-acetylmuramic acid by reducing the double bond in the enol ether structure [25]. Inhibition of the MurB enzyme reduces or blocks the synthesis of peptidoglycan, resulting in incomplete structure of the bacterial cell wall; this eventually leads to the production of lytic bacteria under the pressure of permeation [26]. Thus, down-regulation of

the murB and murF genes implies suppressed LGG cell membrane biosynthesis, to some extent, when cocultured with E.coli.

Metabolism refers to the basic physiological processes that maintain a living organism. Coculture of LGG microcapsules with E.coli was associated with down-regulation of metabolism-related genes. Acetate presumably provides a relevant nutrient for Enterobacteria was well as other bacteria [27][28]. In E. coli, the primary pathway of acetate production involves two enzymes that are intimately connected to central metabolism, phosphotransacetylase (Pta) and acetate kinase (AckA) [29]. During exponential growth, acetyl-CoA, the product of glycolysis and the consumable substrate for the tricarboxylic acid (TCA) cycle, can be converted into acetylphosphate (AcP) by Pta and then into acetate by AckA. E. coli also takes up acetate, using the Pta-AckA pathway in reverse, resulting in synthesis of acetyl-CoA. This pathway typically operates at high extracellular acetate concentrations (≥ 8 mM) [30]. Disruption of the Pta-AckA pathway during overflow metabolism causes a significant reduction in the growth rate and viability of the bacteria; although, this is not due to intracellular ATP depletion [31][32]. Hence, down-regulation of the ackA gene will affect LGG metabolism.

Conclusion

To the best of our knowledge, the present study is the first published attempt to determine protein expression differences associated with probiotics-E.coli in situ coculture. In this work, we applied the label-free proteomics approach to quantify the E.coli proteome in response to LGG microcapsules in coculture. The proteomic analysis revealed quantitative changes in a total of 1655 and 1431 proteins in E.coli and LGG, respectively. Among them, 19 proteins were not identified and 68 proteins were specifically identified after coculture; for LGG, these numbers were 35 and 15, respectively. Functional characterization of these proteins by GO and KEGG enrichment analysis suggested that coculture of LGG microcapsules with E.coli increased the expression of stress-related genes and decreased the expression of secondary metabolism genes, energy metabolism genes, and protein biosynthesis genes in E.coli and LGG strains. These findings further our understanding of the possible molecular action of LGG microcapsules against E.coli biofilm formation. Our future studies will focus on the analysis of posttranslational modifications of differentially expressed proteins as well as endogenous protein complexes and protein-protein interactions.

Methods

Bacterial strains and materials

The Lactobacillus rhamnosus GG and Escherich coli K12MG165 were obtained from American Type Culture Collection (ATCC 53103 and ATCC 47076). LGG was cultured in a modified MRS broth in which glucose was replaced by galactose with anaerobic at 37℃. E.coli strains were cultured at 37℃ in Luriae Bertani broth [33]. The cell suspension was subsequently used as described below.

Sodium alginate was purchased from the Qingdao Crystal Salt Bioscience and Technology Corporation (Qingdao, Shandong, China). Chitosan was degraded from raw chitosan using the chemical method (Yuhuan Ocean Biomaterials Corporation, China). All other reagents and solvents were analytical reagents and were used without further purification.

Preparation of LGG microcapsules

Preparation of LGG alginate beads using the emulsification/internal gelation technique

The LGG microcapsules were prepared using the emulsification/internal gelation method described previously [34]. In general, sodium alginate powder was dissolved in 0.9% (w/v) NaCl solution to obtain the final concentration of 1.5% (w/v). A cell pellet obtained by centrifugation at 10000 rpm for 5 min. The cells and micro-crystalline $CaCO_3$ powder were finely dispersed in sterile sodium alginate solution. Then, the alginate–calcium salt-cell suspension was added in 200 mL liquid paraffin containing 0.5% (v/v) Span 85 in a turbine reactor under stirring at 200 rpm for 30 min. After 30 min emulsification, glacial acetic acid was added for gelification. Then, 500 mL deionized water was added into the above emulsion under stirring for 30 min at a speed of 200 rpm. The cell entrapped calcium alginate beads with an initial cell number of about 1.0×10^6 CFU/mL bead were then rinsed with 1% (v/v) Tween 80 solution and distilled water, and were stored in water at 4℃.

Preparation of LGG alginate-chitosan microcapsules

Chitosan solution was dissolved in 0.1 mol/L acetate buffer. The cell entrapped calcium alginate beads were immersed in 0.5% (w/v) chitosan solution by gently shaking, at a bead/solution ratio of 1:5 (v/v). After rinsing and liquefication for 6 min using 0.055 mol/L sodium citrate, the cell entrapped alginate-chitosan microcapsules were formed.

Preparation of cell samples for proteomic analysis

Briefly, LGG microcapsules were cocultured with planktonic E.coli for 48 h for biofilm inhibition, as reported previously [5]. Then, the biofilms were collected by sonication using high intensity focused ultrasound (UTR2000, Hielscher) (marked as E.coli-B1, E.coli-B2, and E.coli-B3) and were lysed in medium with 4% w/v Sodium Dodecyl Sulfate (SDS), 0.1 mM dithiothreitol (DTT), and 100 mM Tris-HCl, pH 8.2. At the same time, the LGG microcapsules were collected after coculture, and the entrapped LGG cells were released from the microcapsules according to the method previously described [35] (marked as LGG-B1, LGG-B2, and LGG-B3). E.coli pure culture (marked as E.coli-A1, E.coli-A2, and E.coli-A3) and 48 h LGG microcapsules pure culture (marked as LGG-A1, LGG-A2, and LGG-A3) were used as the negative controls.

Protein identification by nanoLC-MS/MS

Precipitated with 100% ethanol (9:1 [v/v]), the protein extracts (100 μg) were resuspended in the denaturation buffer (7 M urea, 2 M thiourea, and 30 mM Tris, pH 8.0) of 100 μL, and conducted with the reduced, alkylated, and in-solution digested procedures with trypsin at a protein:trypsin ratio of 50:1 with the publicized methods [36]. The LTQ-Orbitrap XL and Ultimate 3,000 RSLCnano systems (ThermoFisher Scientific, USA) were used to analyze the trypsin-digested peptides equivalent to 1 μg of each protein

digest using the nanoLC-MS / MS analysis method. The peptide was loaded at a flow rate of 0.05 mL / min onto a 20 mm × 75 μm trap column filled with PepMap100 3 μm C18 resin for 3 minutes. The mobile phase consisted of 98% water, 2% acetonitrile and 0.05% trifluoroacetic acid. Then, the peptides were separated on a 250 mm x 75 μm analytical column packed with PepMap 100 2 μm C18 resin (ThermoFisher Scientific, USA) at a flow rate of 0.3 μL / min, and the temperature was maintained at 40 ° C. The multi-stage gradient from 98% mobile phase A (0.1% formic acid in water) to 50% mobile phase B (0.08% formic acid in 80% acetonitrile and 20% water) is divided into three parts (3–10% B in Within 12 minutes; 10–40% B within 120 minutes; 40–50% B within 10 minutes), which is held at 95% B for 20 minutes, and then rebalanced in 3% B for 15 minutes. Xcalibur 2.1 (ThermoFisher Scientific, USA) was used to control the LTQ-Orbitrap XL. The process was run in a data-related acquisition mode and a measurement scan (m / z 460–2000) was acquired in Orbitrap with a resolution of 60,000. MS / MS spectra were obtained simultaneously on the eight strongest ions obtained from an FT survey scan in an LTQ mass analyzer. Unassigned single-charged precursor ions were neither selected for fragmentation, but were dynamically excluded using 30 seconds (repeated count 1; exclusion list size 500). The debris conditions in LTQ are: a normalized collision energy of 35%, an activation q of 0.25, an activation time of 30 minutes, and a minimum ion selection intensity of 3000 counts.
Database search and statistical analysis of the proteins being identified

The ion currents extracted from the matched peptides[37] were used to import RAW files from the LTQ-Orbitrap into MaxQuant software version 1.5.1.2 (http://www.maxquant.org/). The present study used MaxQuant default parameters for protein identification and label-free quantification (LFQ) by LTQ-Orbitrap MS / MS, including up to two missed trypsin cleavages, variable oxidation of methionine, and cysteine Fixed urea methylation. In addition, this study used MaxQuant default parameters for protein identification and label-free quantification (LFQ) with LTQ-Orbitrap MS / MS, including at most two missed trypsin cleavages, variable oxidation of methionine, and fixed amino methylated cysteine. Peptide map matching and protein identification error detection rates were set to 1%. MaxLFQ is based on a pairwise comparison of unique and razor peptide strengths with a minimum ratio of 2 [38] for peptide strength determination and normalization. The processing of the ProteinGroups.txt output file generated by MaxQuant is as follows. Normalized label-free quantitative (LFQ) peptide intensity values and the number of razors and unique peptides for each identified protein were included in the Perseus software of 1.5.031 version (http://perseus-framework.org/). The proteome (prefixed with CON_) identified as a potential contaminant and proteins recognized by site identification only or reverse database matching are eliminated, and the remaining observed intensity values were conducted with log2 conversion. Measures were taken to filter the proteins to eliminate proteins detected in fewer than nine biological samples or based on a single matching peptide. Based on the normal distribution of protein abundance, the missing value is replaced by the random intensity value of the low-abundance protein. In order to identify proteins with the abundance being changed significantly after heat treatment, a two-way t-test using multiple hypothesis tests using Benjamini Hochberg correction was applied. Unless otherwise stated, the statistical significance was determined by using a 1% FDR threshold. A second data set is generated by filtering to include proteins detected in at least three replicates of any biological sample in

order to detect proteins that are only present at moderately high abundance at one or two specific growth temperatures. By filtering to include proteins detected in at least three replicates of any biological sample, a second dataset was produced, so as to enable detection of proteins existing at moderate or high abundance only at one or two specific growth temperatures. UniProt [39] was used to identify homologs of unidentified proteins and, where appropriate, using BLASTN's protein sequence analysis method, using the Kyoto Encyclopedia of Genes and Genomes (KEGG) [40] and National Biotechnology Information Center (NCBI) to determine putative identity [41].
Bioinformatic analysis of identified proteins and prediction of promoters in intergenic regions

Functional profiling of the identified proteins was performed according to their molecular functions GO category based on the functional annotations of E.coli and LGG [42].

The regulated trends of secreted proteins were visualized with the use of a heat-map constructed using Heml (version 1.0.1). Hierarchical clustering analysis was performed with the average linkage method using Heml software. The quantitative heat map displays the mean quantitative value for each protein, previously calculated with Scaffold software. The mass spectrometry proteomics data have been deposited into the ProteomeXchange Consortium via the PRIDE [43] partner repository with the dataset identifier PXD007097.
Total RNA isolation and RT-PCR

LGG microcapsules were cocultured with planktonic E.coli for 48 h. The cells were then pelleted by centrifugation at 5000 rpm for 5 min at 4 °C and were resuspended in 1 mL TRIzol (Invitrogen, Carlsbad, CA) for total RNA isolation, according to the manufacturer's protocol. Residual genomic DNA was then removed by treating isolated RNA with the Turbo DNAfree kit (Ambion, Austin, TX). Then, cDNA was synthesized using PrimeScript RT Master Mix (Takara), according to the manufacturer’s instructions. qRT-PCR amplifications were performed with at least three biological replicates using 2 × SYBR Premix Ex TaqTM II (DRR081A, Takara) with a Stratagene MX3000P (Agilent Technologies, CA, USA). The housekeeping gene 16S rRNA was used as control for normalization. The qRT-PCR primers are provided in Table S3. The data were normalized against 16S rRNA and the p-values from student's t-tests are reported as follows: * ≤ 0.05, ** ≤ 0.01, and *** ≤ 0.001.

Supplementary Materials

Table S1. Most highly differentially up-regulated and down-regulated proteins in E.coli after coculture.
Table S2. Most highly differentially up-regulated and down-regulated proteins in LGG after coculture.
Table S3. Primers used in this study.

Declarations

Ethics approval and consent to participate

Not applicable.

Consent for publication

Not applicable.

Availability of data and materials

The datasets generated and/or analysed during the current study are available in the [figshare] repository, [10.6084/m9.figshare.11923542]

Competing interests

The authors declare that they have no competing interests.

Funding

The materials used in this manuscript were supported by the National Natural Science Foundation of China (grant numbers 81601734); The proteomic analysis work was supported by the National Natural Science Foundation of China (grant numbers 81873156) and the Liaoning Provincial Natural Science Foundation of China (grant number 20180530062) supported the publishing charges.

Authors' contributions

Song HY and Shang D designed and planned the study. Lou N and Liu JianJ conducted experiments. Xiang H contributed analytical tools and analyzed the data. Song HY wrote the manuscript. All authors were involved in writing the manuscript and all made substantial contributions to the content and approved the final manuscript.

Acknowledgements

Not applicable.

References

1. Monnappa AK, Dwidar M, Seo JK, Hur JH, Mitchell RJ. Bdellovibrio bacteriovorus inhibits Staphylococcus aureus biofilm formation and invasion into human epithelial cells. Sci Rep. 2014; 4: 3811. https://doi.org/10.1038/srep03811
2. Hetrick EM, Shin JH, Paul HS, Schoenfisch MH. Anti-biofilm efficacy of nitric oxide-releasing silica nanoparticles. Biomaterials. 2009; 30(14): 2782-2789. http://doi: 10.1016/j.biomaterials.2009.01.052
3. Beloin C, Roux A, Ghigo JM. Escherichia coli biofilms. Curr Top Microbiol Immunol. 2008; 322: 249-289. https://doi.org/10.1007/978-3-540-75418-3_12
4. Matsuda Y, Cho O, Sugita T, Ogishima D, Takeda S. Culture supernatants of Lactobacillus gasseri and L. crispatus inhibit Candida albicans biofilm formation and adhesion to HeLa cells. Mycopathologia. 2018; 183(4): 691-700. https://doi.org/10.1007/s11046-018-0259-4
5. Song HY, Zhang JB, Qu JL, Liu JJ, Yin PY, Zhang GX, Shang D. Lactobacillus rhamnosus GG

microcapsules inhibit Escherichia coli biofilm formation in coculture. Biotechnol Lett. 2019; 41(8-9): 1007-1014. https://doi.org/10.1007/s10529-019-02694-2
6. Silva JC, Gorenstein MV, Li GZ, Vissers JP, Geromanos SJ. Absolute quantification of pro-teins by LCMSE: a virtue of parallel MS acquisition. Mol Cell Proteomics. 2006; 5(1): 144-156. https://doi.org/10.1074/mcp.M500230-MCP200
7. Rasmussen RV, Fowler VG, Skov R, Bruun NE. Future challenges and treatment of Staphylo-coccus aureus bacteremia with emphasis on MRSA. Future Microbiol. 2011; 6(1): 43-56. https://doi.org/10.2217/fmb.10.155
8. Grundmann H, Aires-de-Sousa M, Boyce J, Tiemersma E. Emergence and resurgence of meti-cillin-resistant Staphylococcus aureus as a public-health threat. Lancet. 2006; 368(9538): 874-885. https://doi.org/10.1016/S0140-6736(06)68853-3
9. Vieco-Saiz N, Belguesmia Y, Raspoet R, Auclair E, Gancel F, Kempf I, Drider D. Benefits and inputs from lactic acid bacteria and their bacteriocins as alternatives to antibiotic growth pro-moters during food-animal production. Front Microbiol. 2019; 10: 57. https://doi.org/10.3389/fmicb.2019.00057
10. Webb ME, Smith AG, Abell C. Biosynthesis of pantothenate. Nat Prod Rep. 2004; 21(6): 695-721. http://doi.org/ 10.1039/b316419p
11. Fouad WM, Altpeter F. Transplastomic expression of bacterial L-aspartate-alpha-decarboxylase enhances photosynthesis and biomass production in response to high temperature stress. Transgenic Res. 2009; 18(5): 707-718. https://doi.org/10.1007/s11248-009-9258-z
12. Lee J, Hiibel SR, Reardon KF, Wood TK. Identification of stress-related proteins in Esche-richia coli using the pollutant cis-dichloroethylene. J Appl Microbiol. 2010; 108(6): 2088-2102. https://doi.org/10.1111/j.1365-2672.2009.04611.x
13. Juárez-Rodríguez MD, Torres-Escobar A, Demuth DR. ygiW and qseBC are co-expressed in Aggregatibacter actinomycetemcomitans and regulate biofilm growth. Microbiology. 2013; 159(Pt 6): 989-1001. https://doi.org/10.1099/mic.0.066183-0
14. Rigel NW, Ricci DP, Silhavy TJ. Conformation-specific labeling of BamA and suppressor analysis suggest a cyclic mechanism for β-barrel assembly in Escherichia coli. Proc Natl Acad Sci U S A. 2013; 110(13): 5151-5156. https://doi.org/10.1073/pnas.1302662110
15. Liu S, Wu N, Zhang S, Yuan Y, Zhang W, Zhang Y. Variable persister gene interactions with (p)ppGpp for persister formation in Escherichia coli. Front Microbiol. 2017; 8: 1795. https://doi.org/10.3389/fmicb.2017.01795
16. Xu X, Jiao L, Feng X, Ran J, Liang X, Zhao R. Heterogeneous expression of DnaK gene from Alicyclobacillus acidoterrestris improves the resistance of Escherichia coli against heat and acid stress. AMB Express. 2017; 7(1): 36. https://doi.org/10.1186/s13568-017-0337-x
17. Grudniak AM, Wlodkowska J, Wolska KI. Chaperone DnaJ influences the formation of bio-film by Escherichia coli. Pol J Microbiol. 2015; 64(3): 279-283. http://www.pjm.microbiology.pl/archive/vol6432015279.pdf
18. Dahl JU, Koldewey P, Salmon L, Horowitz S, Bardwell JC, Jakob U. HdeB functions as an acid-protective chaperone in bacteria. J Biol Chem. 2015; 290(16): 9950. https://doi.org/10.1074/jbc.A114.612986

19. Diether M, Nikolaev Y, Allain FH, Sauer U. Systematic mapping of protein-metabolite inter-actions in central metabolism of Escherichia coli. Mol Syst Biol. 2019; 15(8): e9008. https://doi.org/10.15252/msb.20199008
20. Kriegeskorte A, Block D, Drescher M, Windmüller N, Mellmann A, Baum C, Neumann C, Lorè NI, Bragonzi A, Liebau E, Hertel P, Seggewiss J, Becker K, Proctor RA, Peters G, Kahl BC. Inactivation of thyA in Staphylococcus aureus attenuates virulence and has a strong impact on metabolism and virulence gene expression. MBio. 2014; 5(4): e01447-14. https://doi.org/10.1128/mBio.01447-14
21. Yee R, Cui P, Shi W, Feng J, Zhang Y. Genetic screen reveals the role of purine metabolism in Staphylococcus aureus persistence to rifampicin. Antibiotics (Basel). 2015; 4(4): 627-642. https://doi.org/10.3390/antibiotics4040627
22. Truong QL, Cho Y, Barate AK, Kim S, Watarai M, Hahn TW. Mutation of purD and purF genes further attenuates Brucella abortus strain RB51. Microb Pathog. 2015; 79: 1-7. https://doi.org/10.1016/j.micpath.2014.12.003
23. Karl HS, Otto K. Peptidoglycan types of bacterial cell walls and their taxonomic implications. Bacteriol Rev. 1973; 37(2): 258. https://mmbr.asm.org/content/37/2/258.long
24. Benson TE, Walsh CT, Hogle JM. (1994) Crystallization and preliminary X-ray crystallo-graphic studies of UDP-N-acetylenolpyruvylglucosamine reductase. Protein Sci. 1994; 3(7): 1125-1127. https://doi.org/10.1002/pro.5560030718
25. Lees WJ, Benson TE, Hogle JM, Walsh CT. □E□-enolbutyryl-UDP-N-acetylglucosamine as a mechanistic probe of UDP-N-acetylenolpyruvylglucosamine reductase □MurB□. Biochemistry. 1996; 35(5): 1342-1351. https://doi.org/10.1021/bi952287w
26. Weidel W, Pelzer H. Bagshaped macromolecules - a new outlook on bacterial cell walls. Adv Enzymol Relat Subj Biochem. 1964; 26: 193-232. https://doi.org/10.1002/9780470122716.ch5
27. Rowland I, Gibson G, Heinken A, Scott K, Swann J, Thiele I, Tuohy K. Gut microbiota func-tions: Metabolism of nutrients and other food components. Eur J Nutr. 2018; 57(1): 1-24. https://doi.org/10.1007/s00394-017-1445-8
28. Wolfe AJ. The acetate switch. Microbiol Mol Biol Rev. 2005; 69(1): 12-50. https://doi.org/10.1128/MMBR.69.1.12-50.2005
29. De Mets F, Van Melderen L, Gottesman S. Regulation of acetate metabolism and coordination with the TCA cycle via a processed small RNA. Proc Natl Acad Sci U S A. 2019; 116(3): 1043-1052. https://doi.org/10.1073/pnas.1815288116
30. Enjalbert B, Millard P, Dinclaux M, Portais JC, Létisse F. Acetate fluxes in Escherichia coli are determined by the thermodynamic control of the Pta-AckA pathway. Sci Rep. 2017; 7: 42135. https://doi.org/10.1038/srep42135
31. Marshall DD, Sadykov MR, Thomas VC, Bayles KW, Powers R. Redox imbalance underlies the fitness defect associated with inactivation of the Pta-AckA pathway in Staphylococcus au-reus. J Proteome Res. 2016; 15(4): 1205-1212. https://doi.org/10.1021/acs.jproteome.5b01089
32. Sadykov MR, Thomas VC, Marshall DD, Wenstrom CJ, Moormeier DE, Widhelm TJ, Nuxoll AS, Powers R, Bayles KW. Inactivation of the Pta-AckA pathway causes cell death in Staphy-lococcus aureus. J Bacteriol. 2013; 195(13): 3035-3044. https://doi.org/10.1128/JB.00042-13

33. Dekeersmaecker SC, Vanderleyden J. Constraints on detection of autoinducer-2 (AI-2) sig-naling molecules using Vibrio harveyi as a reporter. Microbiology. 2003; 149 (Pt 8): 1953-1956. https://doi.org/10.1099/mic.0.C0117-0
34. Song HY, Yu WT, Liu XD, Ma XJ. Improved probiotic viability in stress environments with post-culture of alginate-chitosan microencapsulated low density cells. Carbohydr Polym. 2014; 108: 10-16. https://doi.org/10.1016/j.carbpol.2014.02.084
35. Xue WM, Yu WT, Liu XD, Wang HW, Ma XJ. Chemical method of breaking the cell-loaded sodium alginate/chitosan microcapsule. Chemical Journal of Chinese Universities. 2004; 25, 1342-1346. http://10.1016/j.jco.2003.08.015
36. Wilson R, Diseberg AF, Gordon L, Zivkovic S, Tatarczuch L, Mackie EJ, Gorman JJ, Bateman JF. Comprehensive profiling of cartilage extracellular matrix formation and maturation using sequential extraction and label-free quantitative proteomics. Mol Cell Proteomics. 2010; 9(6): 1296-1313. https://doi.org/10.1074/mcp.M000014-MCP201
37. Cox J, Neuhauser N, Michalski A, Scheltema RA, Olsen JV, Mann M. Andromeda: a peptide search engine integrated into the MaxQuant environment. J Proteome Res. 2011; 10(4): 1794-1805. https://doi.org/10.1021/pr101065j
38. Cox J, Hein MY, Luber CA, Paron I, Nagaraj N, Mann M. Accurate proteome-wide label-free quantification by delayed normalization and maximal peptide ratio extraction, termed MaxLFQ. Mol Cell Proteomics. 2014; 13(9): 2513-2526. https://doi.org/10.1074/mcp.M113.031591
39. UniProt Consortium T. UniProt Consortium: the universal protein knowledgebase. Nucleic Acids Res. 2018; 46(5): 2699. https://doi.org/10.1093/nar/gky092
40. Kanehisa M, Goto S. KEGG: Kyoto encyclopedia of genes and genomes. Nucleic Acids Res. 2000; 28(1): 27-30. https://doi.org/10.1093/nar/28.1.27
41. NCBI Resource Coordinators. Database resources of the national center for biotechnology information. Nucleic Acids Res. 2017; 45(D1): 12-17. https://doi.org/10.1093/nar/gkw1071
42. Hochwind K, Weinmaier T, Schmid M, van Hemert S, Hartmann A, Rattei T, Rothballer M. Draft genome sequence of Lactobacillus casei W56. J Bacteriol. 2012; 194(23): 6638. https://doi.org/10.1128/JB.01386-12
43. Vizcaı´no JA, Csordas A, del-Toro N, Dianes JA, Griss J, Lavidas I, Mayer G, Perez-Riverol Y, Reisinger F, Ternent T, Xu QW, Wang R, Hermjakob H. 2016 update of the PRIDE database and its related tools. Nucleic Acids Res. 2016; 44(D1): 447-456. https://doi.org/10.1093/nar/gkv1145

Figures

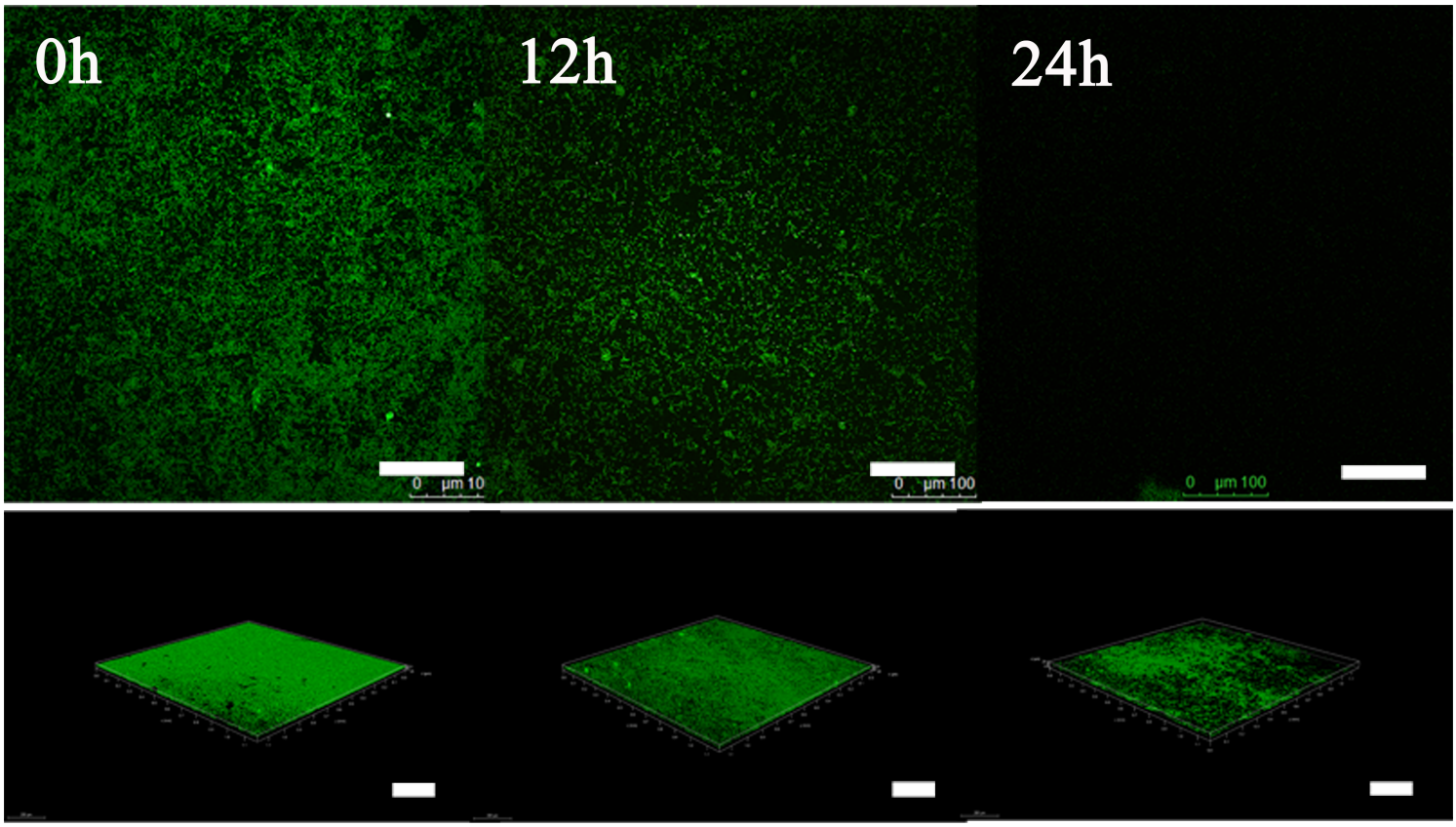

Figure 1

Confocal sections of biofilms of E.coli before and after coculture.

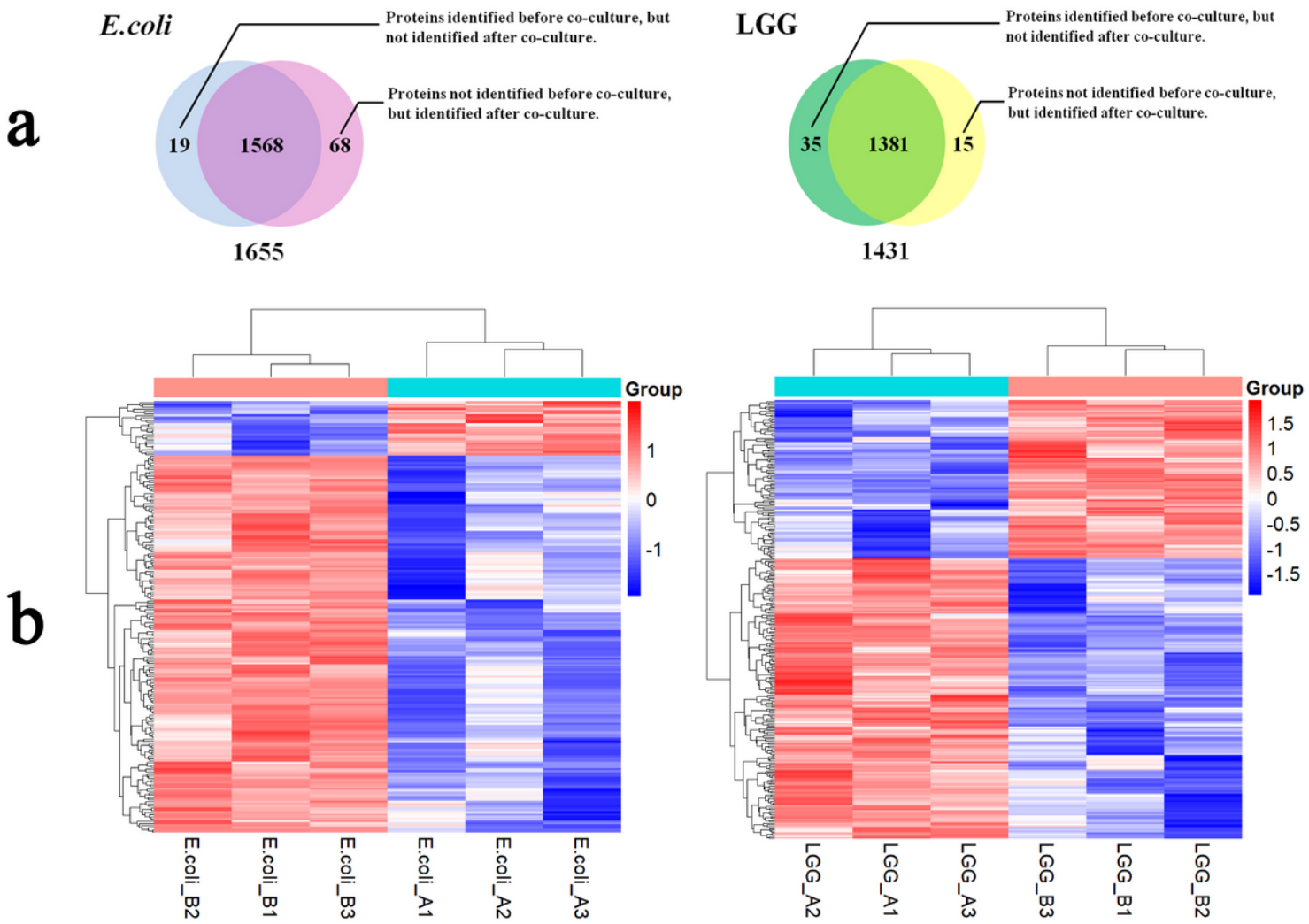

Figure 2

(A) Venn diagram summarizing the overlap proteins and differential proteins identi-fied and quantified between before coculture and after coculture groups. (B) Hierar-chical cluster of proteins differentially expressed in (a) E.coli before coculture (E.coli-A1, 2, 3) and after coculture (E.coli-B1, 2, 3). (b) LGG before coculture (LGG-A1, 2, 3) and after coculture (LGG-B1, 2, 3). Red represent high expression and blue represent low expression. Two main clusters of proteins can be observed, one up-regulated (right) and other down-regulated (left).

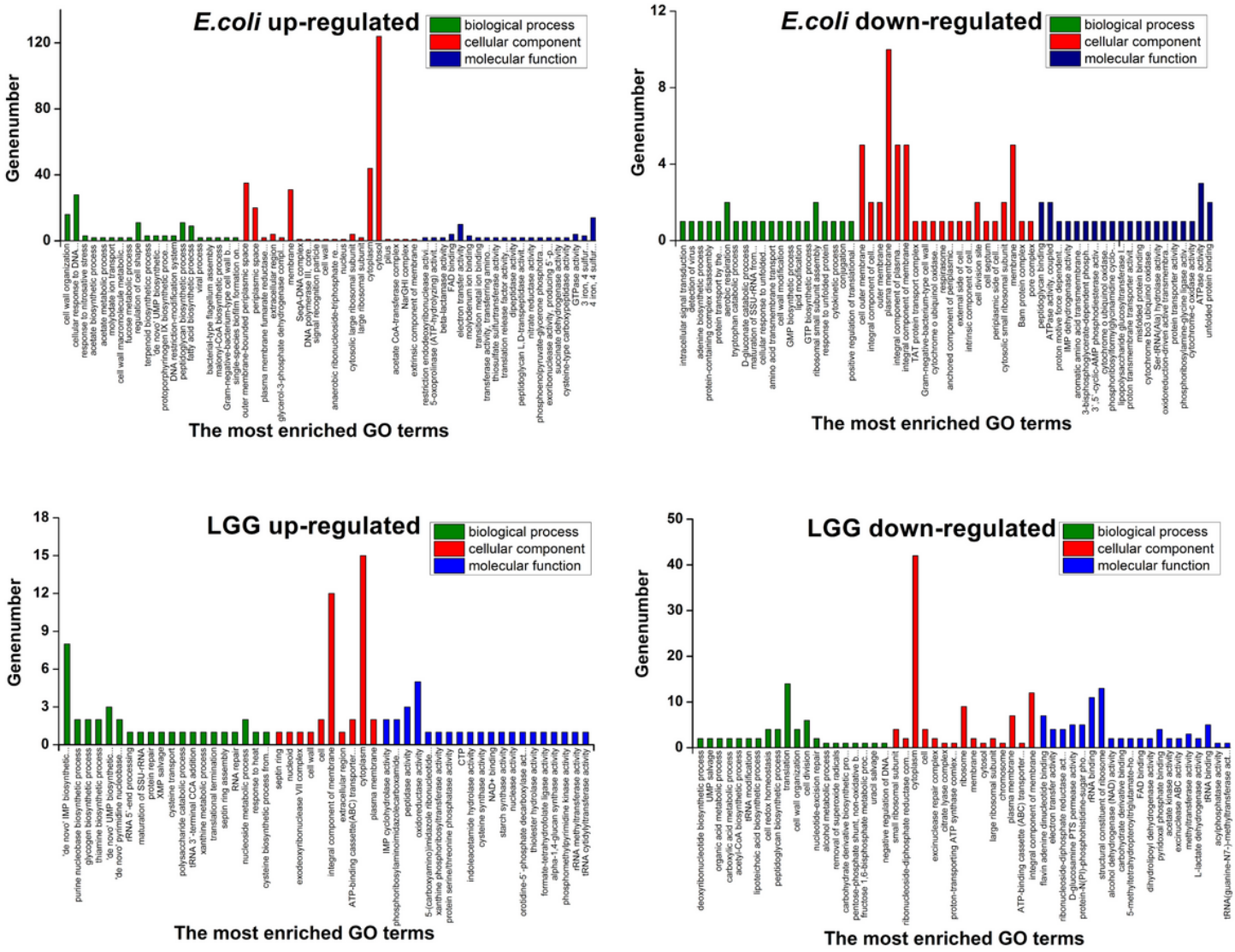

Figure 3

Annotation of overall regulated bacterial protein functions by enrichment of Gene Ontology (GO) terms. Based on the classifications of GO annotation, the overall bacterial functions were categorized into biological process, molecular function, and cellular component, and displayed in histogram format. The numbers of GO terms for each of the three categories are shown, whereas the proportion of each specific subcategory is also provided. Subcategories with GO terms less than 1% are classi-fied as “other”.

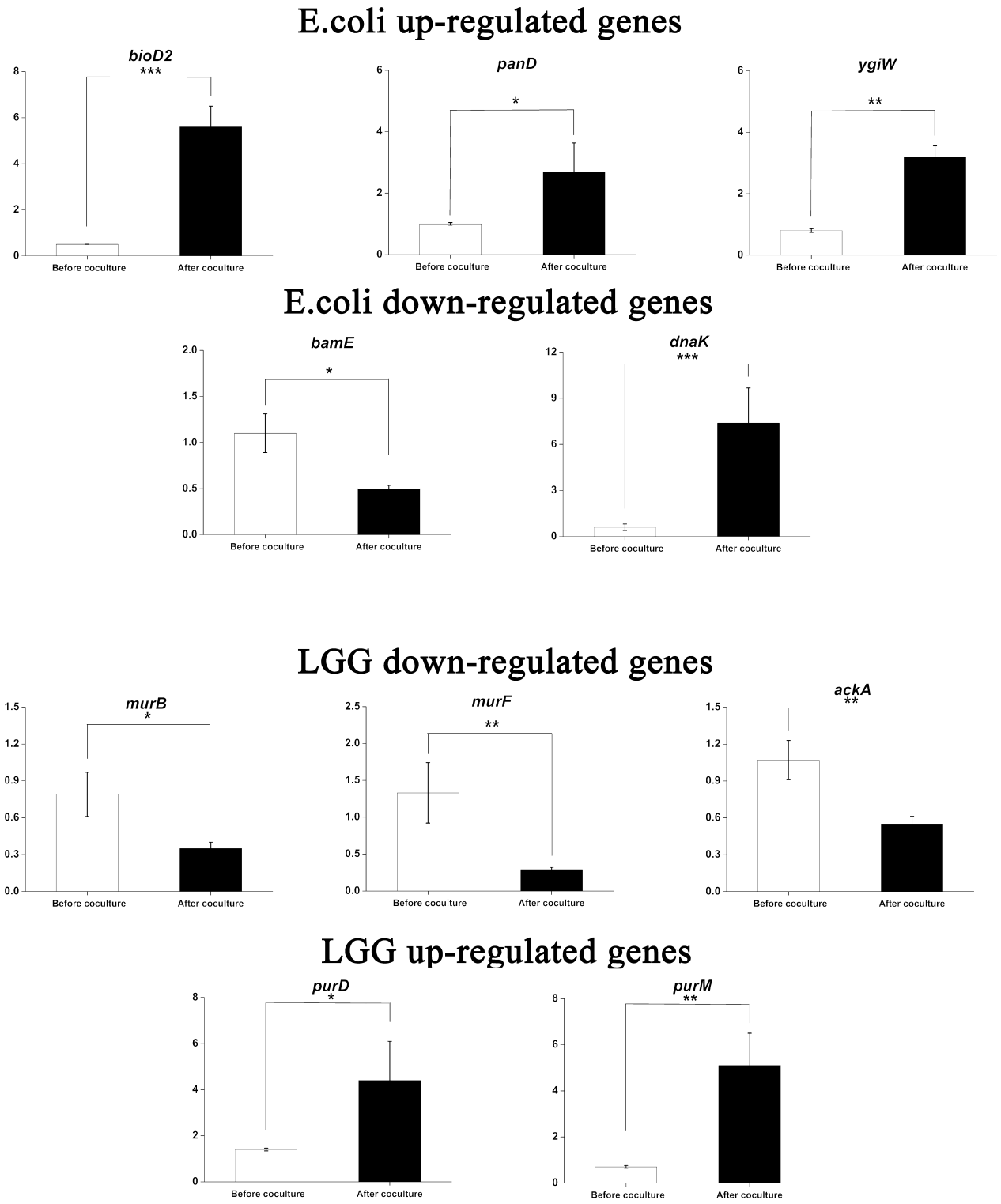

Figure 4

Relative mRNA expression of select targets from global proteomics analysis. Total RNA isolated from coculture treatment or pure culture of the E.coli and LGG was reversed transcribed and cDNAs were quantified by qRT-PCR using target-specific primers. The data represents the mean ± SD of triplicate experiments normalized with 16S RNA. Statistically significant differences between coculture treatment

and pure culture-treatment as determined by Student's t-test analysis (unpaired, two-tailed) is represented as *p≤ 0.5, **p≤ 0.1 and ***p≤ 0.01.

Supplementary Files

This is a list of supplementary files associated with this preprint. Click to download.

- supplementarymaterials.docx